Influence of Gold Nanoparticles on the Characteristics of Plasma Display Panels

Woo Hyun Kim, Kwan Hyun Cho, Kyung Cheol Choi, *Member, IEEE*, Do Youb Kim, and O Ok Park

Abstract—This paper proposes a modified alternating current plasma display panel (PDP) in which gold nanoparticles are incorporated into a bare MgO layer to enhance the performance of the protective layer. The proposed structure's ion-induced secondary electron yield, which is expressed in a gamma value (γ value) is greater than that of a bare MgO layer; as a result, the operating voltage decreases by 10 V to 20 V. The integration of emitted infrared (IR) light and the power density consumed by the discharge current are both increased, but the ratio of increment is greater for the case of the IR light. Consequently, IR efficacy is increased. The IR response time of the sustain discharge and the address discharge time lag are reduced by the enhanced wall charge accumulation characteristic and the exoelectron emission property. The results of ultraviolet photoelectron spectroscopy show that a MgO layer with Au nanoparticles has a lower work function than a conventional bare MgO layer. Furthermore, the structure that is not flattened by nanoparticles seems to enhance the secondary electron emission property of the MgO protective layer. Consequently, the γ value is enhanced by the two reasons previously mentioned.

Index Terms—Gold nanoparticles, MgO protective layer, nanometer-scale bump, plasma display panels (PDPs).

I. INTRODUCTION

ALTERNATING-CURRENT plasma display panels (ac PDPs) have great marketability in the large flat-panel display market, owing to their fast operating speed and simple manufacturing process. Furthermore, ac PDPs, with a diagonal larger than 50 in, make a conspicuous figure in the 3-D display market.

An ac PDP has a lower luminous efficacy than other flat-panel displays such as a liquid-crystal display or an organic lighting-emitting diode. In spite of numerous efforts to overcome this weakness, researchers are still looking for an innovative way of improving the luminous efficacy of ac PDPs [1]. In the past years, researchers have tried methods such as modifying the electrode structure, changing the mixture of gases, and reforming the driving scheme [2], [3]. On a recent study, in the spotlight is the modification of a protective layer for a higher rate of secondary electron emission (SEE). Many studies on a protective layer have focused on the important role of SEE in terms of discharge characteristics. There are several examples: the RF plasma treatment of a MgO layer, the addition of some ions to a MgO layer, the hybrid plasma display with ZnO, and a double protective layer [4]–[7].

There have also been several studies on the formation of a bumpy structure on the front plate of ac PDPs. Changing the surface morphology to a microscale capillary or bowl structure was proposed for the purpose of low operating voltage, fast discharge time lag, and high vacuum ultraviolet efficacy [8], [9].

In line with previous works [4]–[9], this paper proposes that a modified protective layer be incorporated with Au nanoparticles. Chemically synthesized Au nanoparticles, with a diameter in the range of 50–100 nm, are inserted in a MgO protective layer by means of an air-spray method. These conductive metal nanoparticles form nanoscale bumps on the protective layer, producing positive effects on the discharge characteristics. In addition, metal particles themselves are helpful to improve discharge characteristics by affecting the amount of wall charge on the protective layer. This study is the first attempt to insert metal nanoparticles and form nanoscale bumps on a MgO protective layer. This paper investigates the improved discharge characteristics and examines the reasons for these phenomena.

II. EXPERIMENTAL SETUP

A. Chemical Synthesis of Au Nanoparticles

Au nanoparticles with a diameter in the range of 50–100 nm are synthesized by a chemical method. In a typical method, 3.5 ml of N,N-Dimethylformamide (DMF) and 1.4 ml of water are added to a DMF solution with 0.1 ml of 94.2-mmol hydrogen tetrachloroaurate trihydrate ($HAuCl_4$) and 7 ml of 1.46-mmol polyvinylpyrrolidone (PVP). This solution is then capped and heated in an oil bath at 120 °C for 2 h with stirring. The final solution is subsequently cooled and purified by centrifugation for washing of the PVP and collection of the Au nanoparticles. The key reaction mechanism in the formation of the Au nanoparticles is given as follows:

$$2HAuCl_4 + 3HCON(CH_3)_2 + 3H_2O$$

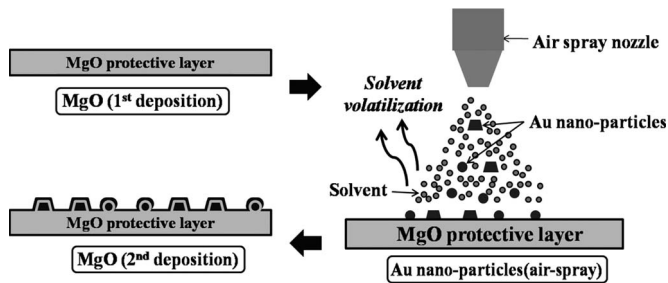$$\leftrightarrow 2Au + 3(CH_3)_2NCOOH + 8H^+ + 8Cl^-.$$

Fig. 1. Process flow diagram of the formation of Au nanoparticles on a MgO protective layer.

The size and shape of the Au nanoparticles are determined by the reaction time. In this experiment, with a reaction time of approximately 8 min, the Au nanoparticles are in the range of 50–100 nm; some of the particles are octahedrons, and some are dodecahedrons.

Finally, the collected Au nanoparticles are dispersed in a volatile solvent, i.e., ethanol, so that they can be sprayed on a protective layer of MgO [10].

B. Fabrication of a Bumpy MgO Protective Layer

Fig. 1 shows a process flow diagram of the formation of Au nanoparticles on a MgO protective layer. First, the MgO layer is deposited by electron-beam (E-beam) evaporation. Au nanoparticles with a diameter in the range of dozens of nanometers are then dispersed in ethanol and deposited on the MgO layer by air-spray method. The solution is sprayed by an air-blowing process at room temperature under ambient pressure. Thus, the fabrication process is simple. As soon as the solvent reaches the MgO layer, it disappears into the air immediately because of its volatile characteristic. The Au metal nanoparticles are the only substance that remains on the target substrate. The proposed structure is completed when a second MgO layer is deposited by E-beam evaporation.

Fig. 2 shows a tilted cross-sectional image of the proposed protective layer structure after 6 h of aging. With a size range of 50–100 nm, the Au nanoparticles are distributed uniformly on the MgO surface. The bumpy structure is observed without any prominent damage after the annealing and aging processes. Hence, the morphology change and Au nanoparticles themselves are not greatly affected by the heating and plasma treatments.

C. Test Panel Fabrication and Measurement Setup

A 4-in diagonal panel is fabricated for the purpose of measuring the discharge characteristics. The size of the individual cells is 1080 μm $\times$ 360 μm, which corresponds to a 42-in video graphics array resolution; the coplanar gap between the common electrode and the scan electrode is 80 μm; the width of the ITO electrode is 200 μm; and the width of the Ag bus electrode is 60 μm. The barrier rib is of the stripe type and has a height of 180 μm. The discharge gas consists of Ne + 4%Xe at 450 Torr. The MgO layer deposited before the insertion of Au nanoparticles is 490 nm thick, whereas the MgO layer deposited after the insertion of Au nanoparticles is 5 nm.
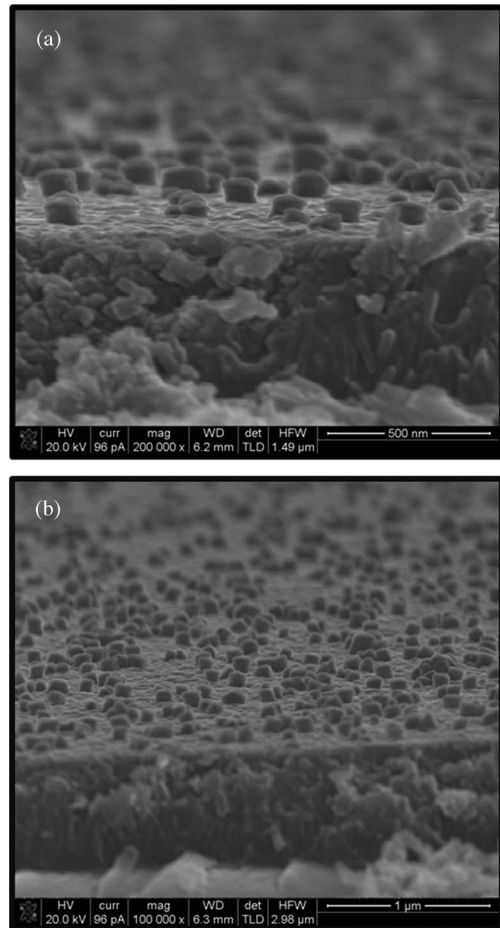

Fig. 2. Tilted cross-sectional scanning electron microscopy images of Au nanoparticles inserted in the MgO protective layer after 6 h of aging. (a) Tilted at an angle of 5°. (b) Tilted at an angle of 10°.
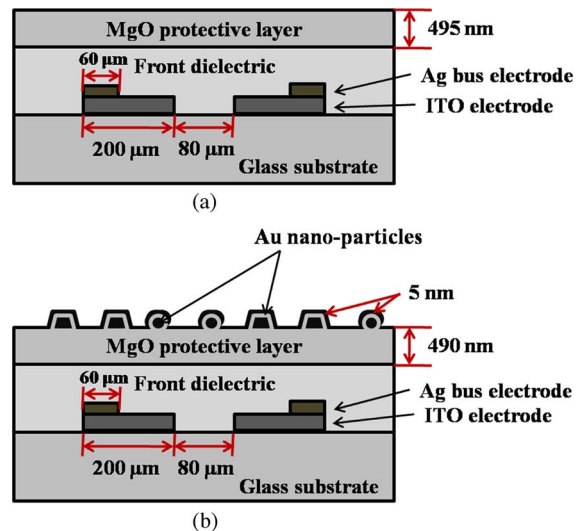

Fig. 3. Schematic diagram of a front plate. (a) Conventional structure. (b) Structure incorporated with Au nanoparticles.

Fig. 3 shows a cross-sectional schematic diagram of the front plate of both a conventional MgO protective layer and a MgO protective layer incorporated with Au nanoparticles. The Au nanoparticles are sprayed on half the test panel for comparison
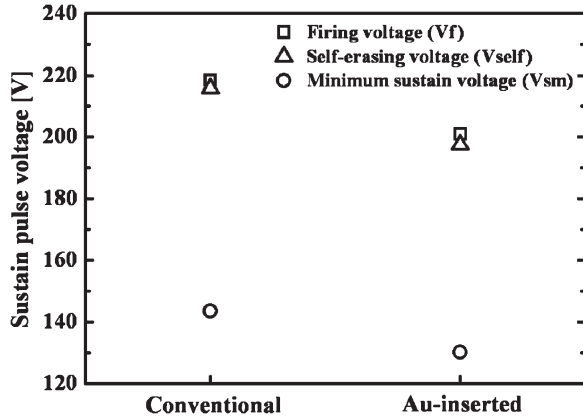
Fig. 4.   Firing voltage, self-erasing voltage, and minimum sustain voltage for a conventional MgO protective layer and a MgO protective layer incorporated with Au nanoparticles.

Fig. 5.   Results of γ-focused ion beam measurements of the γ values for a conventional MgO protective layer and a MgO protective layer incorporated with Au nanoparticles.

of the discharge characteristics with a reference material in the same environment.

A photosensor (Hamamatsu, C6386) was used to measure the infrared (IR) integration data. The numerically calculated power density and IR efficacy are based on measurements of the sustain pulse voltage, the driving current, and the IR integration values. The aforementioned photosensor and an oscilloscope (Tektronix DPO4034) were used to measure the IR response time and the address time lag.

III. RESULTS AND DISCUSSION

Fig. 4 shows the firing voltages, minimum sustain voltages, and self-erasing voltages of the conventional MgO layer and the MgO layer incorporated with Au nanoparticles. The firing and self-erasing voltages are about 17–18 V less in the structure incorporated with Au nanoparticles than in the conventional structure. In addition, a 13-V decrement of the minimum sustain voltage is observed in the structure incorporated with Au nanoparticles than in the conventional structure. The reason for the decreased operating voltage is investigated here in relation to the SEE property.

Fig. 5 shows the gamma value (γ value) of the conventional MgO protective layer and the MgO protective layer incorporated with Au nanoparticles. The γ value, which represents the ion-induced secondary electron yield, is measured with a γ-focused ion beam system [11]. The results show that the γ values of the proposed structure are higher than those of the conventional structure for all values of the acceleration voltage. The reduction in the firing voltage and the minimum sustain voltage is explained by increased γ values, which indicate that the SEE is enhanced. An explanation of the increment in the SEE is given at the end of this paper. One weakness of PDPs is the high operating voltage, which is attributed to the additional electronic circuits used to drive the high voltage. However, the problem can be alleviated by the insertion of Au nanoparticles in the MgO protective layer.

In particular, the fact that the difference in the voltage reduction between the firing voltage and the minimum sustain voltage is 5 V means that th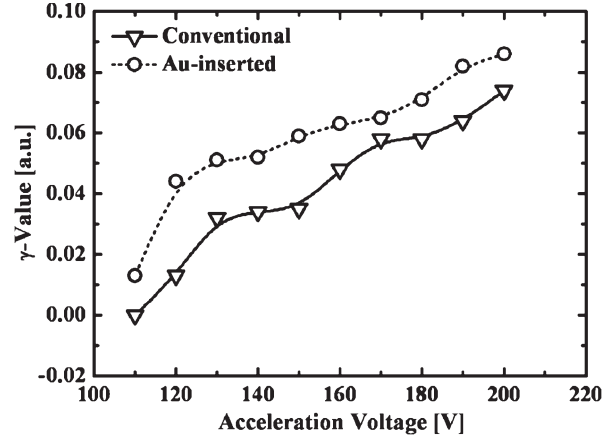e static sustain margin is not significantly reduced. Although the MgO was mixed with an alkaline earth oxide CaO or SrO for the purpose of producing a protective layer with a high γ value, the decrement in the static sustain margin was a significant problem [12]. The method of mixing MgO with an alkaline earth oxide to induce a lower work function or electron affinity leads to a higher conductivity of the protective layer. As a result, the amount of wall charge accumulated on the protective layer is reduced, and the static sustain margin consequently becomes smaller [5]. In general, a strong correlation exists between the surface conductivity and the amount of wall charge on the protective layer. However, in the proposed structure, the inserted metal particles affect the amount of wall charge on the protective layer, although the resultant effect on surface conductivity is not expected to be significant. As shown in Fig. 2, the effect is not significant, because the particles are isolated by oxide material and separated from each other by a distance in the range of dozens of nanometers. The decrement of the static sustain margin is consequently small.

Fig. 6 shows the integration of the emitted IR, the power density consumed by the discharge current, the IR efficacy, and the increment ratio of these parameters for a conventional MgO protective layer and a MgO protective layer incorporated with Au nanoparticles. Fig. 6(a) and (b) confirms that the IR integration and the power density are greater in the MgO protective layer incorporated with Au nanoparticles than in the conventional MgO protective layer. As shown in Fig. 6(c), the numerical calculation of the data on the IR integration and power consumption confirms that the proposed structure yields a higher level of IR efficacy. The increment in the IR integration value increases the IR efficacy; inversely, the increment in the power density reduces the IR efficacy. In conclusion, the IR integration has a higher increment ratio than that of the power density, which means that, as shown in Fig. 6(d), there is a higher level of IR efficacy. Because of the lack of efficacy data for the conventional MgO layer under a sustain pulse voltage of 150 V, the increment ratio data of the IR efficacy are obtained through comparisons with the maximum IR efficacy of the conventional structure. In general, a higher level of IR efficacy
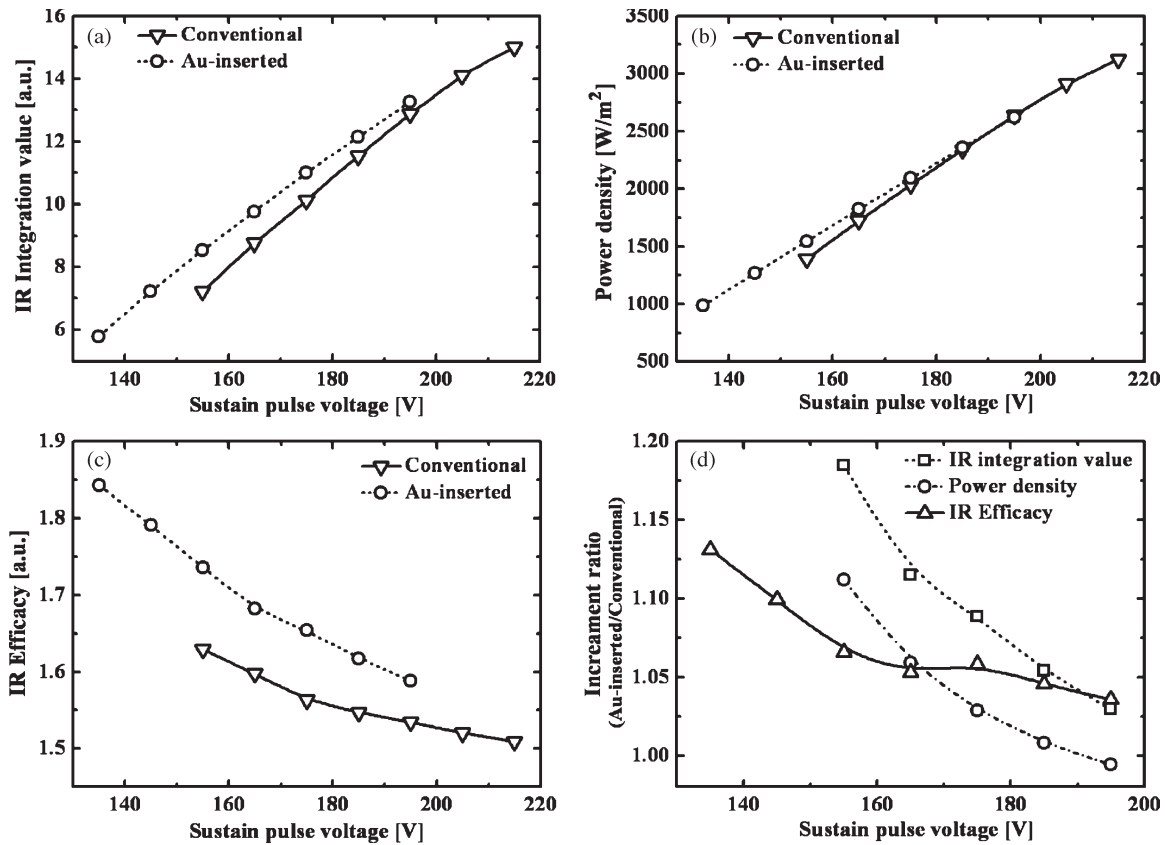
Fig. 6. (a) Integration value of IR emission. (b) Power density consumed by the discharge current. (c) IR efficacy for a conventional MgO protective layer and a MgO protective layer incorporated with Au nanoparticles. (d) Increment ratio of the proposed MgO protective layer, compared with the conventional MgO protective layer for (a), (b), and (c).

is obtained for a lower sustain pulse voltage; furthermore, as shown in Fig. 6(c) and (d), a higher level of IR efficacy is observed when the voltage is less than 150 V. A lower operating voltage means that simple driving circuits can be used in a device and that a higher level of IR efficacy can be achieved in a low-voltage region.

The visible light emitted by phosphor is important in display devices. In this case, the Au nanoparticles must reach an optimal density level to produce a higher level of luminous efficacy, because they can screen visible light emissions; moreover, similar results are obtained for the luminous efficacy of red phosphor [13].

Fig. 7 shows the IR response time of the sustain discharge of a conventional MgO protective layer and a MgO protective layer incorporated with Au nanoparticles. The time interval between 10% of the peak voltage and 10% of the peak IR value is measured as the response time or the time lag [14]. The data are measured 500 times and averaged for each sustain pulse voltage. The IR response time of a MgO protective layer incorporated with Au nanoparticles is smaller than that of a conventional MgO protective layer. This outcome means that the discharge is faster in the sustain period. The IR response time of the sustain discharge is affected by the applied voltage, which refers to the strength of the electric field on the discharge cell. The applied voltage on a cell seems to increase, because the wall charge is increased by the metal particles, and a higher electric field can be locally induced around the nanoscale
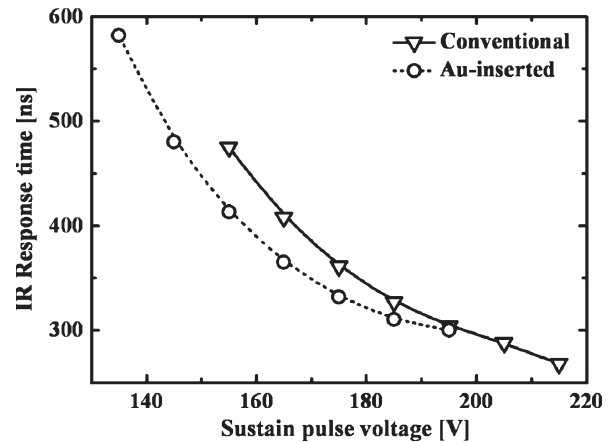

Fig. 7. IR response time of the sustain discharge for a conventional MgO protective layer and a MgO protective layer incorporated with Au nanoparticles.

bumps; as a result, this process can induce a faster discharge than a bare MgO protective layer [7], [14].

Fig. 8(a) shows the driving voltage waveform of the measurements of the address time lag, and Fig. 8(b) shows a Laue plot of the address time lag. Owing to a difference in the operating voltage, the voltage levels of the reset waveform and the sustain pulse are optimized for each structure. The designed voltage levels, which are enumerated alphabetically in Fig. 8(a), are listed in Table I. A thousand items of data were collected at
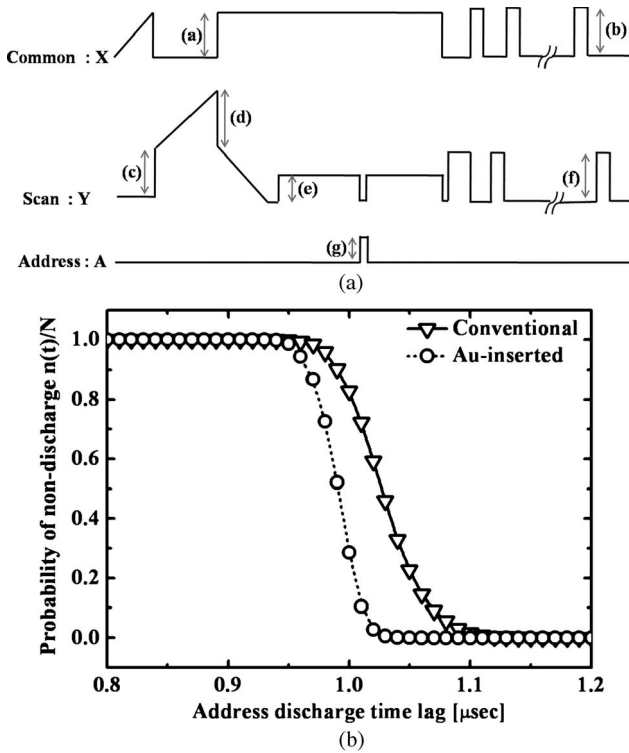
Fig. 8. (a) Driving waveform. (b) Laue plot of the address discharge time lag for a conventional MgO protective layer and a MgO protective layer incorporated with Au nanoparticles.

TABLE I
VOLTAGE LEVELS, AS MARKED IN FIG. 8(a)

Panels	(a)	(b)	(c)	(d)	(e)	(f)	(g)
Conventional	185	185	185	165	100	185	75
Au-inserted	160	175	160	140	100	175	75

different positions on four occasions, resulting in a total of 4000 items of data for each structure. These data are demonstrated in Fig. 8(b). In Fig. 8(b), the address time lag is observed to be lower in a MgO protective layer incorporated with Au nanoparticles than in a conventional MgO protective layer. The proposed structure appears to show an earlier starting point in the decrement because of the reduced formative time lag; there is also a drastic decrement in the graph because of the reduced statistical time lag. In general, a formative delay is related to the strength of the electric field, and a statistical delay is strongly related to the amount of initial electrons or seed electrons [15]. In view of the previously discussed reasons for the reduced IR response time of the sustain discharge, the formative time lag is expected to be reduced by the increased wall charge and the locally induced electric field. As shown in Fig. 9, the enhanced exoelectron emission (EEE) property of the structure incorporated with Au nanoparticles increases the number of seed electrons in account of the reduced work function and consequently reduces the statistical time lag [16]. As a result, the address time lag, which is the sum of the formative time lag and the statistical time lag, is reduced by 130 ns in the proposed structure.
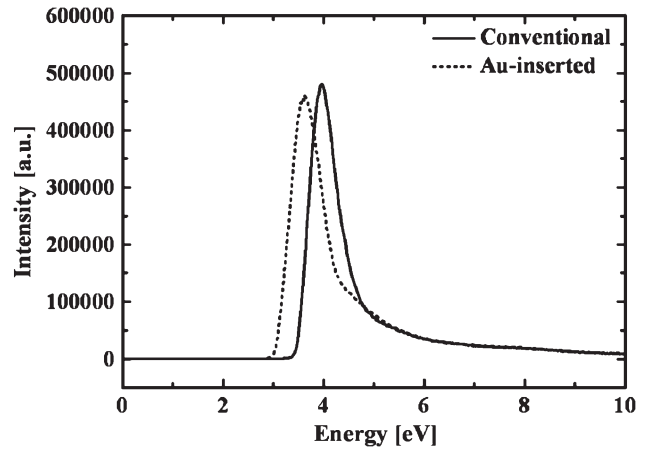

Fig. 9. UPS data for a conventional MgO protective layer and a MgO protective layer incorporated with Au nanoparticles.

The reasons for the SEE enhancement are now investigated. Fig. 9 shows the data of ultraviolet photoelectron spectroscopy (UPS); the data indicate the work function of the surface material in a conventional MgO protective layer and a MgO protective layer incorporated with Au nanoparticles. The test sample is fabricated on a silicon substrate to prevent any charging effect. In addition, the MgO layer that is deposited before the Au nanoparticles are added is 7 nm thick, whereas the MgO layer deposited after the Au nanoparticles are added is 5 nm. Furthermore, the sample is bonded to a metal chuck with conductive carbon tape to produce a pathway of positive charges. The work function is derived from the value of the x-axis at the peak point, which is 3.61 eV for the conventional MgO protective layer and 3.22 eV for the proposed MgO protective layer. As a result, when the Au nanoparticles are inserted, the work function of the proposed structure falls by about 0.4 eV, and the SEE property is consequently enhanced [11], [17]. In addition, the nonflat-surface morphology, which is induced by the nanometer-scale bumps, is expected to enhance the SEE property [18]. Thus, as shown in Fig. 5, the γ value is increased because of the two reasons previously mentioned. The reason of the decrease in the work function is not proven, so further investigation is needed.

X-ray diffraction (XRD) and cathodoluminescence (CL) were used to confirm the change in the crystal orientation and the density of the oxygen vacancy. Fig. 10(a) shows the XRD data of a conventional MgO protective layer and a MgO protective layer incorporated with Au nanoparticles. The position and intensity of the peaks are similar for both the conventional and proposed structures, except for the existence of the Au (111) peak. There is consequently no change in the crystal orientation when the Au nanoparticles are added. Fig. 10(b) shows the CL data of the bare MgO layer and the two MgO layers sprayed with Au nanoparticles for 15 and 30 s, respectively. The density of the oxygen vacancy is qualitatively estimated in terms of the intensity of the CL data. The differences in the intensity of the bare MgO sample and the Au incorporated samples are in an error range of measurement, and there is no apparent trend with regard to the density of the Au nanoparticles. Thus, when Au nanoparticles are added, there is no significant change in the density of the oxygen vacancy.
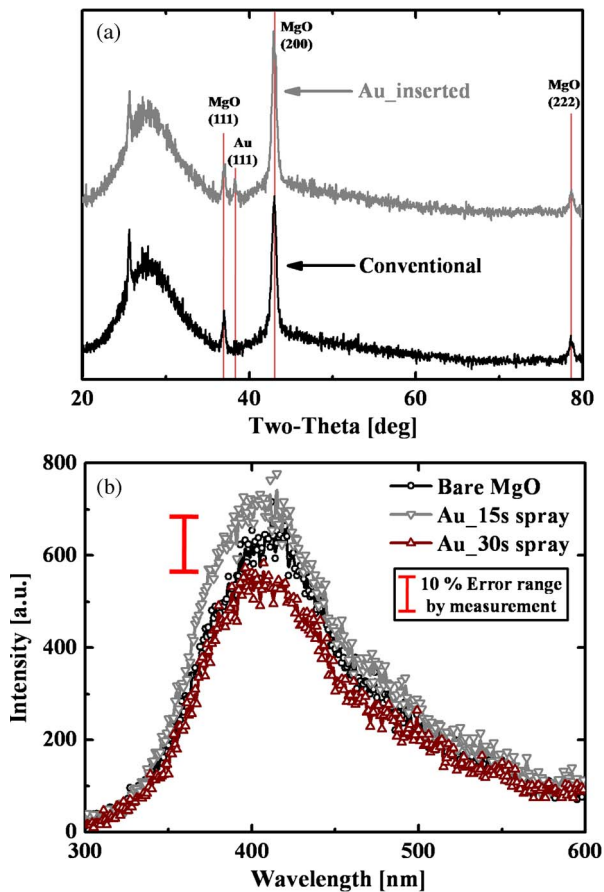
Fig. 10. (a) XRD data of a conventional MgO protective layer and a MgO protective layer incorporated with Au nanoparticles. (b) CL data for a bare MgO layer and a MgO layer sprayed with Au nanoparticles for 15 and 30 s, respectively.

IV. CONCLUSION

This paper proposes a modified PDP with a MgO protective layer incorporated with Au nanoparticles. Compared with a conventional bare MgO protective layer, the proposed structure achieves a lower operating voltage, a higher IR efficacy, a faster IR response time of the sustain discharge, and a shorter address time lag. The Au nanoparticles reduce the work function of the MgO and form the nanometer-scale bumps on the MgO surface. Consequently, an increase in the SEE and EEE properties enhances the discharge characteristics. In addition, although the discharge characteristics are enhanced by the incorporation of Au nanoparticles, more in-depth consideration should be given between the enhancement of the discharge characteristics and the loss of the fabrication cost.

REFERENCES

[1] J. P. Boeuf, "Plasma display panels: Physics, recent developments and key issues," *J. Phys. D, Appl. Phys.*, vol. 36, no. 6, pp. R53–R79, Feb. 2003.

[2] K. C. Choi, N. H. Shin, S. C. Song, J. H. Lee, and S. D. Park, "A new AC plasma display panel with auxiliary electrode for high luminous efficacy," *IEEE Trans. Electron Devices*, vol. 54, no. 2, pp. 210–218, Feb. 2007.

[3] G. Oversluizen, M. Klein, S. de Zwart, S. van Heusden, and T. Dekker, "Improvement of the discharge efficiency in plasma displays," *J. Appl. Phys.*, vol. 91, no. 4, pp. 2403–2408, Feb. 2002.

[4] C. S. Park, H. S. Tae, B. K. Park, E. Y. Jung, and J. C. Ahn, "Enhancement of discharge characteristics using RF-plasma treatment on MgO layer in 50-in. Full-HD AC-PDPs," in *Proc. SID Dig.*, 2009, pp. 363–366.

[5] S. I. Ahn, S. E. Lee, S. H. Ryu, K. C. Choi, S. J. Kwon, and H. Uchiike, "A study on the secondary electron emission from Na-ion-doped MgO films in relation to the discharge characteristics of plasma display panels," *Thin Solid Films*, vol. 517, no. 5, pp. 1706–1709, Jan. 2009.

[6] K. W. Whang, H. Y. Jung, T. H. Lee, and H. W. Cheng, "High luminous efficacy and low driving voltage PDP with SrO-MgO double protective layer," in *Proc. IMID Dig.*, 2009, pp. 173–176.

[7] S. H. Yoon, H. S. Yang, and Y. S. Kim, "Ordered growth of ZnO nanorods for fabrication of a hybrid plasma display panel," *Nanotechnology*, vol. 18, no. 20, p. 205 608, Apr. 2007.

[8] S. H. Park, T. S. Cho, K. H. Becker, and E. E. Kunhardt, "Capillary plasma electrode discharge as an intense and efficient source of vacuum ultraviolet radiation for plasma display," *IEEE Trans. Plasma Sci.*, vol. 37, no. 8, pp. 1611–1614, Aug. 2009.

[9] K. H. Cho, S. I. Ahn, W. H. Kim, and K. C. Choi, "AC plasma display panel with irregular micro-scale holes in the front dielectric layer," in *Proc. IMID Dig.*, 2009, pp. 711–712.

[10] D. Y. Kim, S. H. Im, O. O. Park, and Y. T. Lim, "Evolution of gold nanoparticles through Catalan, Archimedean, and Platonic solids," *CrystEngComm*, vol. 12, pp. 116–121, 2010.

[11] J. Y. Lim, J. S. Oh, B. D. Ko, J. W. Cho, S. O. Kang, G. S. Cho, H. S. Uhm, and E. H. Choi, "Work function of MgO single crystals from ion-induced secondary electron emission coefficient," *J. Appl. Phys.*, vol. 94, no. 1, pp. 764–769, Jul. 2003.

[12] T. Shinoda, H. Uchiike, and S. Andoh, "Low-voltage operated AC plasma-display panels," *IEEE Trans. Electron Devices*, vol. ED-26, no. 8, pp. 1163–1167, Aug. 1979.

[13] W. H. Kim, K. H. Cho, K. Y. Yang, C. S. Choi, S. I. Ahn, D. Y. Kim, O. O. Park, and K. C. Choi, "AC plasma display panel with gold nanoparticles inserted into an MgO protective layer," in *Proc. SID Dig.*, 2010, pp. 1588–1590.

[14] S. H. Son, Y. S. Park, S. C. Bae, and S. Y. Choi, "Application of hollow channel between sustain electrodes to improve discharge characteristics in alternating current plasma display panels," *Appl. Phys. Lett.*, vol. 80, no. 10, pp. 1719–1721, Mar. 2002.

[15] J. S. Kim, J. H. Yang, T. J. Kim, and K. W. Whang, "Comparison of electric field and priming particle effects on address discharge time lag and addressing characteristics of high-Xe content AC PDP," *IEEE Trans. Plasma Sci.*, vol. 31, no. 5, pp. 1083–1090, Oct. 2003.

[16] I. S. Choi, K. J. Suh, M. S. Yoo, and E. G. Heo, "Study of the correlation between doped MgO workfunction and address delay," in *Proc. IMID Dig.*, 2008, pp. 961–964.

[17] Y. Motoyama, Y. Murakami, M. Seki, T. Kurauchi, and N. Kikuchi, "SrCaO protective layer for high-efficiency PDPs," *IEEE Trans. Electron Device*, vol. 54, no. 6, pp. 1308–1314, Jun. 2007.

[18] J. S. Oh and E. H. Choi, "Ion-induced secondary electron emission coefficient (γ) from MgO protective layer with microscopic surface structures in alternating current plasma display panels," *Jpn. J. Appl. Phys.*, vol. 43, no. 9A/B, pp. 1154–1155, 2004.

Woo Hyun Kim received the B.S. and M.S. degrees in electrical engineering, in 2008 and 2010, respectively, from Korea Advanced Institute of Science and Technology, Daejeon, Korea, where he is currently working toward the Ph.D. degree in electric engineering with the Department of Electrical Engineering.

His research interests include microplasma display and plasmonics.

Kwan Hyun Cho received the B.S. degree in electrical engineering from Kyungpook National University, Daegu, Korea, in 2005 and the M.S. degree in electrical engineering, in 2007, from Korea Advanced Institute of Science and Technology, Daejeon, Korea, where he is currently working toward the Ph.D. degree in electric engineering with Department of Electrical Engineering.

His research interests include microplasma and plasmonics for display applications.

Kyung Cheol Choi (M'04) received the B.S. degree and the M.S. and Ph.D. degrees in plasma engineering from Seoul National University, Seoul, Korea, in 1986, 1988, and 1993, respectively.

From 1993 to 1995, he was with the Institute for Advanced Engineering, Seoul, where his work focused on the design of display devices. From 1995 to 1996, he was a Research Scientist with Spectron Corporation of America, Summit, NJ. From 1996 to 1998, he was a Senior Research Scientist with Hyundai Plasma Display, Hawthorne, NY. From 1998 to 1999, he was a Senior Research Scientist with the Advanced Display R&D Center, Hyundai Electronics Industries, Gyounggi, Korea, where he was involved in the development of a 40-in ac plasma display panel (PDP). From 2000 to 2004, he was an Associate Professor with the Department of Electronics Engineering, Sejong University, Seoul. He was also in charge of the Information Display Research Center supported by the Korean Ministry of Information and Communication. Since 2005, he has been with the Department of Electrical Engineering, Korea Advanced Institute of Science and Technology, Daejeon, Korea, where he was first an Associate Professor and is currently a Professor. Since September 2007, he has been in charge of the Center for Advanced Flexible Display Convergence supported by the Korean Ministry of Education, Science, and Technology. His research interests include flexible displays, PDPs, organic light-emitting diodes, and surface plasmon applications for displays.

Dr. Choi is a member of the Society for Information Display and the Korean Information Display Society. He is an Associate Editor for the *IEEE/OSA Journal of Display Technology*.

Do Youb Kim received the B.S. degree in chemical engineering from Konkuk University, Seoul, Korea, in 2007. He is currently working toward the Ph.D. degree in chemical and biomolecular engineering with the Department of Chemical and Biomolecular Engineering, Korea Advanced Institute of Science and Technology, Daejeon, Korea.

As a visiting student, he joined Prof. Y. Xia's group in biomedical engineering at Washington University, St. Louis, in March 2010. His research interests include the synthesis, analysis, and application of metal nanostructures.

O Ok Park received the Ph.D. degree from Stanford University, Stanford, CA, in 1985.

He is currently a Professor with the Department of Chemical and Biomolecular Engineering, Korea Advanced Institute of Science and Technology (KAIST), Daejeon, Korea. He has been with KAIST as a Professor for the last 25 years. He has authored more than 230 papers with more than 3100 citations. His current research interests include metal nanoparticles, polymer electroluminescence devices, polymer solar cells, colloidal self-assembly and related nanosoft lithography, and polymer nanocomposites.

Prof. Park is a member of the National Academy of Engineering of Korea and the Korean Academy of Science and Technology.